Article

Not peer-reviewed version

Viniferin-Rich Phytocomplex from *Vitis vinifera* L. Plant Cell Culture Mitigates Neuroinflammation in BV2 Microglia Cells

Giacomina Videtta , Chiara Sasia , Sofia Quadrino , Oriana Bertaiola , Chiara Guarnerio , Elisa Bianchi , Giacomo Biagiotti , Barbara Richichi , Stefano Cicchi , Giovanna Pressi , Nicoletta Galeotti *

Posted Date: 2 December 2025

doi: 10.20944/preprints202512.0209.v1

Keywords: *Vitis vinifera* L.; neuroinflammation; microglia; BV2 cells; plant cell culture; cellulose nanocrystal; nanoformulation

Article

Viniferin-Rich Phytocomplex from *Vitis vinifera* L. Plant Cell Culture Mitigates Neuroinflammation in BV2 Microglia Cells

Giacomina Videtta [1], Chiara Sasia [1], Sofia Quadrino [1], Oriana Bertaiola [2], Chiara Guarniero [2], Elisa Bianchi [3], Giacomo Biagiotti [3], Barbara Richichi [3], Stefano Cicchi [3], Giovanna Pressi [2] and Nicoletta Galeotti [1,*]

[1] Department of Neurosciences, Psychology, Drug Research and Child Health (Neurofarba), Section of Pharmacology and Toxicology, Laboratory of Neuroinflammation and Cell Senescence, University of Florence, Viale G. Pieraccini 6, 50139 Florence, Italy

[2] Aethera Biotech Srl, Via Dell'Innovazione n. 1, 36043Camisano Vicentino (VI), Italy

[3] Department of Chemistry "Ugo Schiff," University of Florence, Via della Lastruccia 3–13, 50019 Sesto Fiorentino, Italy

* Correspondence: nicoletta.galeotti@unifi.it

Abstract

Activation of microglia and resulting neuroinflammation are central processes that significantly contribute to neurodegenerative disease progression. Treatments capable of attenuating neuroinflammation are therefore an urgent medical need. *Vitis vinifera* L., cultivated since ancient times for its fruits, is known for its antioxidant and anti-inflammatory activities. However, polyphenols, the main bioactive molecules in *V. vinifera* extracts, vary considerably due to numerous hard-to-control factors, making it difficult to obtain standardized extracts with consistent biological activity. To address this issue, plant cell culture biotechnology was used to produce a highly standardized *V. vinifera* phytocomplex (VP), and its anti-neuroinflammatory profile was investigated in LPS-stimulated microglial cells, an in vitro model of neuroinflammation. VP reduced the LPS-induced pro-inflammatory phenotype, improved cell viability and cell number, attenuated NF-κB activation and ERK1/2 phosphorylation, and increased SIRT1 levels. To overcome VP's poor water solubility, water-soluble, nanocellulose-based formulations containing cellulose nanocrystal (CNC) were developed and tested. VP-CNC formulations markedly reduced the BV2 pro-inflammatory phenotype and increased cell viability under both basal and LPS-stimulated conditions. The nanoformulations also decreased pERK1/2 levels and increased SIRT1 expression, exhibiting biological activities comparable to VP alone. *V. vinifera* phytocomplex derived from plant cell cultures represents an innovative and standardized product with promising antineuroinflammatory properties.

Keywords: *Vitis vinifera* L.; neuroinflammation; microglia; BV2 cells; plant cell culture; cellulose nanocrystal; nanoformulation

1. Introduction

Neuroinflammation is a sustained inflammatory response within the central nervous system (CNS) that refers to an infiltration of immune cells into the CNS [1] and to the activation of CNS resident immune cells, primarily microglia and astrocytes, and non-immune cell types [2,3]. These cells release proinflammatory mediators and reactive oxygen and nitrogen species (ROS, RNS) that initiate and propagate neuroinflammatory responses. Acute neuroinflammation elicits a transient, self-limiting reaction that promotes tissue repair and can serve protective functions. When

 doi:10.20944/preprints202512.0209.v1

unresolved, however, the inflammatory cycle becomes prolonged, leading to chronic neuroinflammation, which is ultimately detrimental to the CNS [3,4].

The immune response is initially triggered by microglial activation. While microglial activity is critical for maintaining brain homeostasis [5–7], excessive or prolonged activation leads to the massive release of proinflammatory mediators that promote CNS damage and influence disease outcomes and pathology [8,9]. Neuroinflammation and microglial activation are central events driving neurodegeneration and have been recognized as major contributors to the progression of several neurodegenerative conditions [2,8,10].

Vitis vinifera L. (grape), cultivated for thousands of years by many civilizations, represents one of the largest fruit crops used for wine, juice, and fresh consumption. Its most important active constituents are phenolic compounds, mainly phenolic acids, flavonoids, proanthocyanidins, and characteristic stilbene derivatives [11]. However, the polyphenol composition of *Vitis vinifera* L. is highly complex, and its content can vary considerably depending on the morphological part examined [12]. It is also influenced by factors such as variety, maturity, post-harvest storage, and environmental parameters including location, light conditions, temperature, nutrition, water availability, microorganisms, and viticultural practices [13], making it difficult to standardize grape-based products.

Vitis vinifera L. has traditionally been used as a laxative and carminative, and as a remedy for colds and flu, wound care, allergies, and bronchitis [14,15]. Experimental studies have shown that bioactive compounds found in grapes exhibit antioxidant, antibacterial, antifungal, antidiabetic, anticancer, and cardioprotective activities [16]. The antioxidant properties of grape polyphenols have also been described within the CNS, where they exert beneficial neuroprotective effects [17,18]. These findings suggest that *Vitis vinifera* L. may play a key role in attenuating neuroinflammation, with potential benefits for neurodegenerative diseases. However, the pharmacological effects of *Vitis vinifera* L. on activated microglia have not been elucidated. Thus, our study aimed to evaluate its modulatory effects on microglia-mediated neuroinflammation in LPS-stimulated microglia.

A promising strategy for generating uniform, contaminant-free plant materials on an industrial scale is the use of in vitro plant cell culture technology. By cultivating plant cells under strictly regulated environmental conditions [19], this method ensures consistent production of bioactive metabolites and avoids the fluctuations typical of conventional plant extracts. Extracts and phytocomplexes produced in this way can be accurately standardized for both primary and secondary metabolites and consistently meet safety requirements due to their absence of contaminants and phytochemical uniformity [20].

Furthermore, this approach helps preserve biodiversity and enhances environmental sustainability by significantly reducing the use of natural resources such as water and soil. It also eliminates seasonal and geographical limitations and improves consumer safety by preventing contamination from heavy metals, pesticides, aflatoxins, and microbial agents, while providing a high degree of standardization.

Our results indicated that a viniferin-rich *Vitis vinifera* L. phytocomplex produced through plant cell culture suppressed the proinflammatory morphology and restored cell viability in LPS-stimulated BV2 microglial cells by inhibiting NF-κB activation and increasing SIRT1 expression.

2. Results

2.1. Characterization of Vitis vinifera L. Standardized Phytocomplex Obtained from Cell Culture Suspensions

2.1.1. Development and Preparation of *V. vinifera* L. Standardized Phytocomplex (VP)

A stable, selected *V. vinifera* L. cell line was generated from black grapes using G0 solid medium (Gamborg B5 supplemented with 20 g/L sucrose, 0.8% (w/v) plant agar, 1 mg/L NAA, 1 mg/L IAA, 1 mg/L K, and a final pH of 6.5). Figure 1 shows the flow chart for the development and preparation of

 doi:10.20944/preprints202512.0209.v1

the standardized *V. vinifera* phytocomplex (VP). After six months of routine subculturing on the same medium, the cells exhibited a pale yellow coloration, a friable texture, and a rapid growth rate, requiring transfer to fresh G0 solid medium every three weeks. The appearance of the stabilized V. vinifera cell line grown on G0 solid medium is shown in Figure 1. Fluorescein diacetate staining revealed both the morphology and viability of the plant cells maintained under these conditions (Figure 1). Optimization of total stilbenoid production in *V. vinifera* suspension cultures was achieved using a G0 liquid medium enriched with a higher sucrose concentration (40 g/L) and supplemented with 7.5 mg/L methyl jasmonate and 25 mM β-cyclodextrin, added three days after fermentation began. Figure 1 also illustrates the appearance of the suspension culture in the optimized liquid medium. Cells cultivated in this medium for 14 days were harvested for phytocomplex preparation.

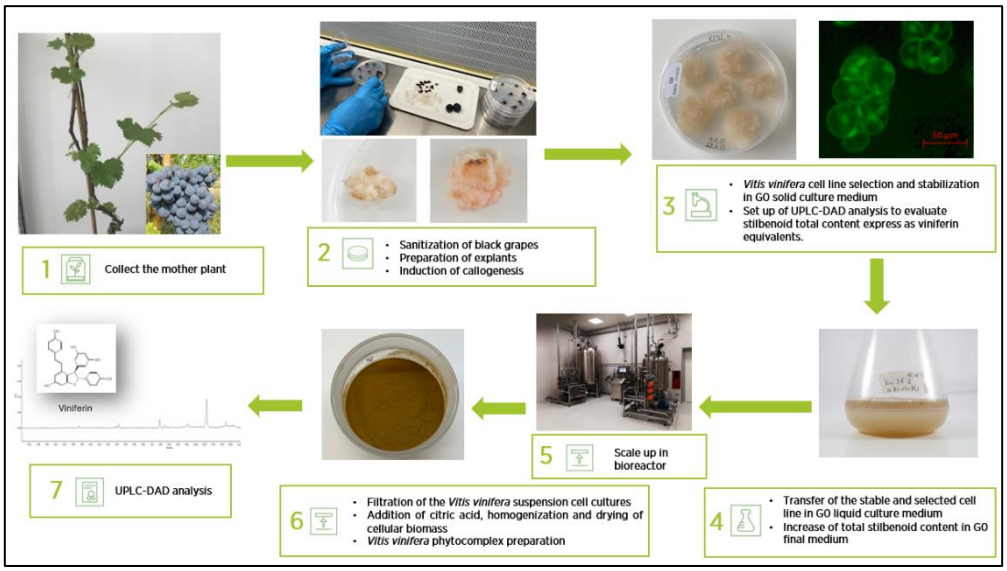

Figure 1. Flow chart of the development and preparation of VP.

2.1.2. UPLC-DAD Analysis

To evaluate the total stilbenoid content in the VP, UPLC-DAD analysis was carried out. The chromatogram recorded at 330 nm is displayed in Figure 2. The total stilbenoid concentration, identified through their characteristic spectral profiles and expressed as viniferin equivalents, was quantified as 0.15 ± 0.02%. The main stilbenoid identified were: viniferin hexoside, viniferin di-hexoside, viniferin tri-hexoside, resveratrol di-hexoside.

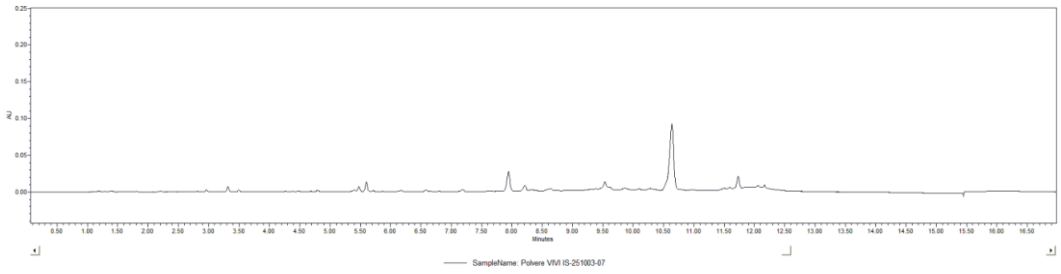

Figure 2. Representative UPLC-DAD chromatogram of VP recorded at 330 nm.

2.2. Effect of VP on an In Vitro Model of Neuroinflammation

2.2.1. Suppression of Microglia Proinflammatory Phenotype by VP

Dose-dependent studies of VP (0.1–100 µg/mL) on BV2 morphology were performed by analyzing cell length (Figure 3A), soma area (Figure 3B), and the percentage of cells in the

 doi:10.20944/preprints202512.0209.v1

proinflammatory state (Figure 3C) under resting conditions. At all concentrations tested, VP did not significantly modify cell morphology compared with the CTRL group.

BV2 cells exhibit distinct morphological phenotypes in resting versus proinflammatory states. Morphological analysis of BV2 cells under LPS stimulation showed a shift toward a stretched and elongated phenotype, as demonstrated by a marked increase in cell length and soma area. VP (0.1–100 µg/mL) reduced cell length (Figure 3D) and cell surface area (Figure 3E). Finally, VP reduced the percentage of cells displaying the elongated proinflammatory phenotype (Figure 3F).

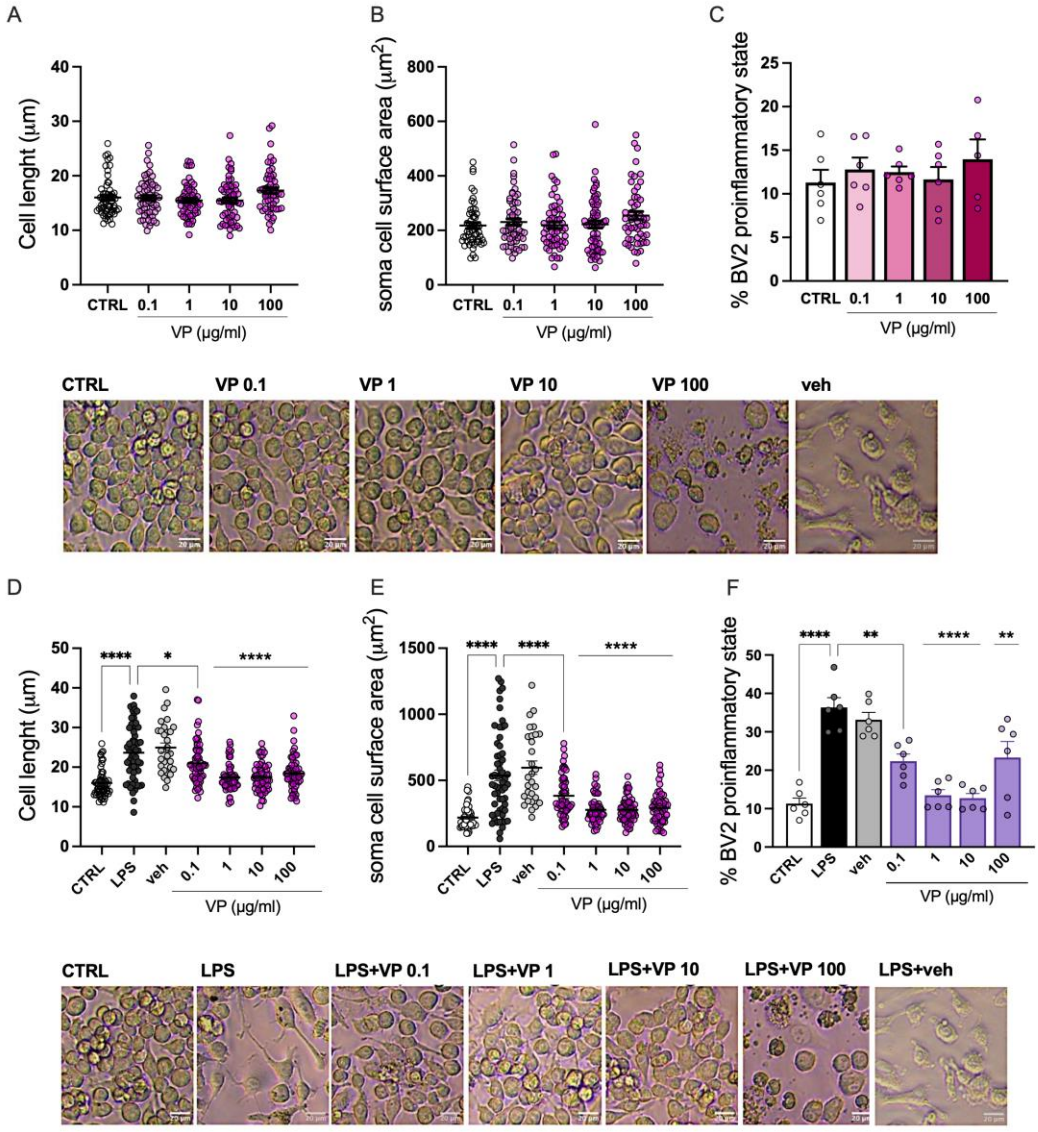

Figure 3. Morphological analysis of microglia cells following VP treatment. No variation was observed on BV2 cell diameter (A), soma surface area (B) and percentage of cells in the proinflammatory state (C) by VP treatment (0.1 -100 µg/mL) at steady state. Dose-dependent attenuation by VP of LPS-induced increase of diameter (D), soma surface area (E) and percentage of cells in the proinflammatory state (F). Representative images of VP-treated unstimulated and stimulate BV2cells. Scale bar: 20 µm. LPS: 250 ng/mL for 24h. Veh = vehicle (50% DMSO). *p<0.05, **p<0.01, ****p<0.0001.

2.2.2. Effect of VP on Microglia Cell Viability

The effect of VP on BV2 cell viability was investigated in the absence and presence of LPS stimulation. Under basal conditions, VP significantly increased cell viability at doses of 0.1, 1, and 10 µg/mL. At the dose of 100 µg/mL, there was a drastic reduction in cell viability, likely due to the

 doi:10.20944/preprints202512.0209.v1

amount of DMSO required to dissolve the phytocomplex (Figure 4A). The effect of VP on cell number was also assessed, showing no effect at doses from 0.1 to 10 µg/mL. Consistent with the cell viability data, the 100 µg/mL dose caused a marked reduction (Figure 4B).

Exposure of BV2 cells to LPS (250 ng/mL for 24 h) significantly reduced both cell viability (Figure 4C) and cell number (Figure 4D). Doses of 0.1, 1, and 10 µg/mL dose-dependently restored cell viability and mitigated the reduction in cell number. The 100 µg/mL dose caused a drastic decrease in both parameters, again due to the DMSO content. Therefore, the 100 µg/mL dose was excluded from further analyses.

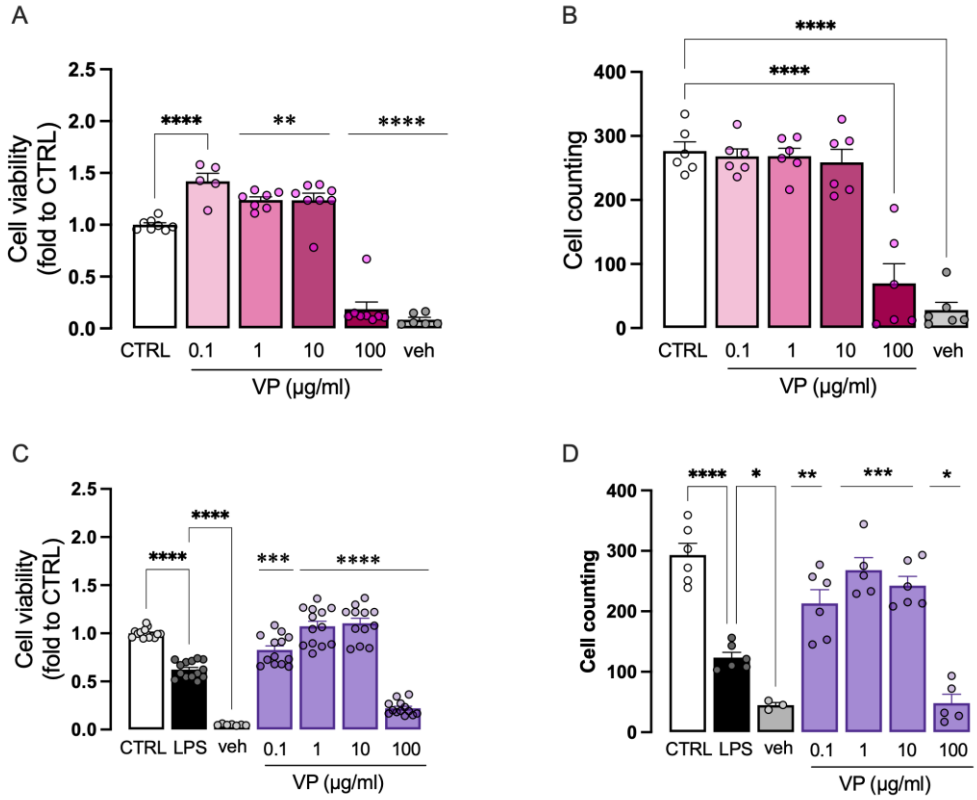

Figure 4. Effect of VP on cell viability. (A)VP (0.1-10) increase of cell viability at resting conditions. VP 100 and veh drop of cell viability. (B) Lack of effect on cell number by VP (0.1-10) at steady state and reduction of cell count by VP 100 and veh. LPS-stimulated cells showed a reduced cell viability (C) and number (D). Dose-dependently reversal of LPS-induced effect by VP 0.1-10 whereas VP 100 showed a toxic activity comparable to veh. LPS: 250 ng/mL for 24h. Veh = vehicle (50% DMSO). *p<0.05, **p<0.01, ***p<0.001, ****p<0.0001.

2.2.3. Modulation of Neuroinflammation Markers by VP

LPS stimulation was associated with robust activation of the NF-κB pathway, as demonstrated by the increased expression of phosphorylated NF-κB (p-NF-κB). In the LPS-treated group, the p-NF-κB/NF-κB ratio was more than twice that of the control group. Doses of 0.1 and 1 µg/mL had no effect, whereas treatment with VP at 10 µg/mL restored the p-NF-κB/NF-κB ratio to basal levels (Figure 5A).

Microglial cells exposed to LPS also showed increased phosphorylation of the MAPK ERK1/2. VP at 0.1 and 1 µg/mL dose-dependently attenuated p-ERK1/2 overactivation, with a peak effect observed at 1 µg/mL. This effect was reduced at higher doses (Figure 5B).

Finally, the effect of VP on SIRT1 levels was assessed. LPS-stimulated cells showed SIRT1 levels comparable to the control group. VP at 0.1 and 1 µg/mL had no effect, whereas treatment with 10 µg/mL resulted in a marked increase in SIRT1 protein expression (Figure 5C).

 doi:10.20944/preprints202512.0209.v1

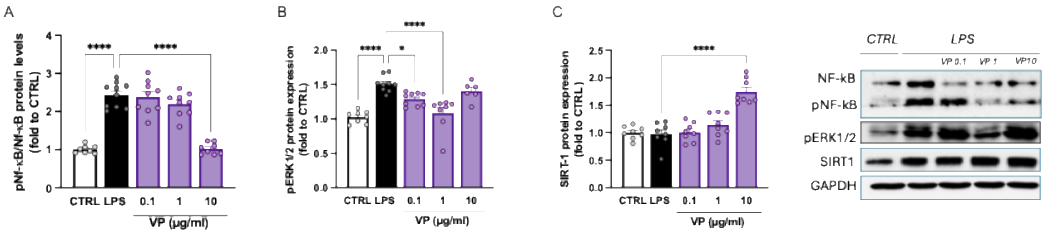

Figure 5. VP-induced modulation of neuroinflammation biomarkers. Dose-dependent reduction of LPS-induced NF-kB activation (A) and ERK1/2 over-phosphorylation. (C) VP-induced increase of SIRT1 protein levels. LPS: 250 ng/mL for 24h. *p<0.05, ****p<0.0001.

2.3. Pharmacological Profile of VP Nanocellulose Formulations

2.3.1. Analysis of VP Nano Cellulose Formulations

VP showed promising anti-neuroinflammatory properties. However, the amount of DMSO required to dissolve the phytocomplex made impossibile to investigate concentrations higher than 10 µg/ml. To overcome the poor water solubility of VP and avoid any potential confounding effect produced by the vehicle, we used water-disperdible nanocellulose formulations as innovative drug-delivery system. This choice is justified by the well known amphiphilic nature of crystalline nanocellulose (from now on CNC) [21,22] which has already found application in the delivery of poorly soluble drugs [23,24]. Specifically, two distinct nano-formulations were used: VP-cellulose nanocrystals (+) (VP-CNC(+)) and VP-sulfated cellulose nanocrystals (-) (VP-CNC(-)) containing VP and CNC in a 1:10 ratio. The two formulations were prepared using a ball milling procedure [25] starting form a commercial form of emisulfated nanocellulose (CNC (-) possessing a negative charge, ζ-potential: (-50.51 ±2.97) mV) or a laboratory prepared derivative (CNC(+) decorated with ammonium ions (ζ-potential: (48.91 ±3.81) mV). Distribution of nanoparticle size is reported in Figure 6.

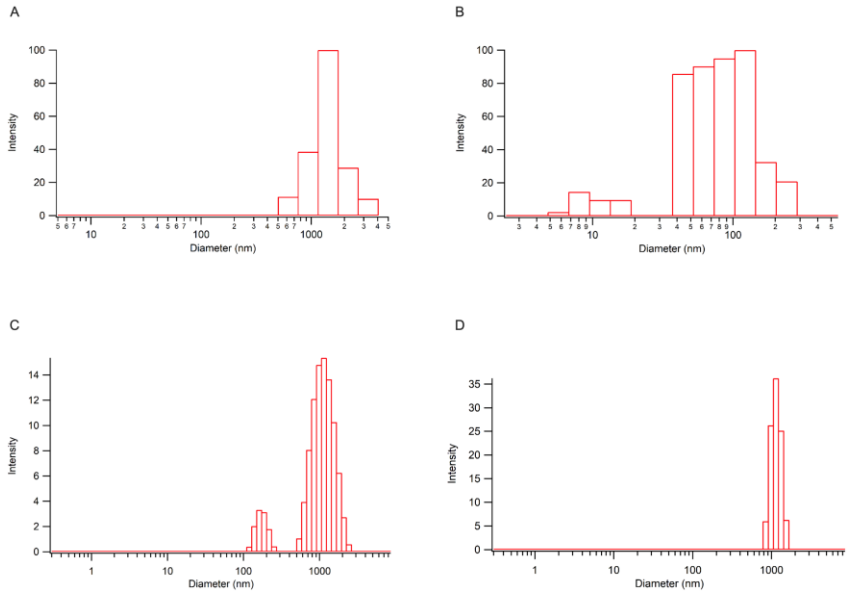

Figure 6. DLS column chart of CNC(+) (A), CNC(-) (B), VP-CNC(+) 1:10 (C), VP-CNC (-) 1:10 (D).

2.3.2. Attenuation of Proinflammatory Morphology by VP-CNC Nanoformulations

Microglia are heterogeneous cells that, even under resting conditions, include a proportion of cells (approximately 15%) in the proinflammatory state. Dose-response curves for the VP-CNC(-) and VP-CNC(+) formulations showed a significant reduction in cell diameter (Figure 7A) and soma area

 doi:10.20944/preprints202512.0209.v1

(Figure 7B) under basal conditions, starting from 0.1 µg/mL. Furthermore, treatment with VP-CNC(-) and VP-CNC(+) reduced the percentage of cells in the proinflammatory state (Figure 7C).

Morphological analysis of LPS-stimulated cells demonstrated that both formulations effectively reduced the LPS-induced increase in cell diameter at all doses tested (Figure 7D) and normalized the soma area (Figure 7E) to basal levels. Both formulations also reduced the LPS-induced increase in the percentage of cells in the proinflammatory state, restoring it to values comparable to the control group (Figure 7F).

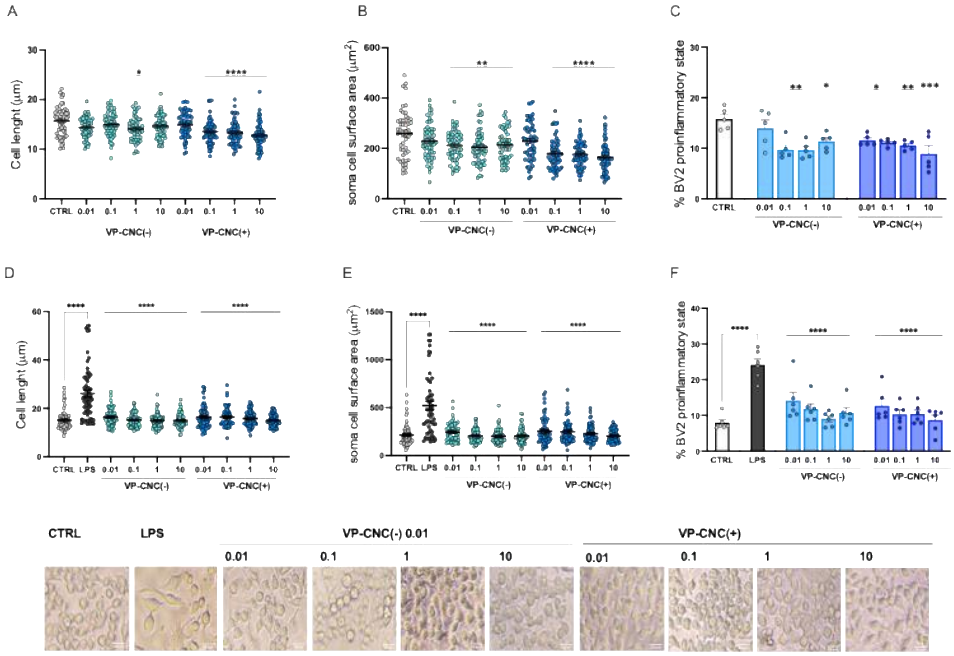

Figure 7. Morphological analysis of microglia cells following VP-CNC treatment. Reduction of BV2 cell diameter (A), soma surface area (B) and percentage of cells in the proinflammatory state (C) by VP-CNC formulations (0.01 -10 µg/ml) at basal conditions. VP-CNC attenuation by of LPS-induced increase of diameter (D), soma surface area (E) and percentage of cells in the proinflammatory state (F). Representative images of VP-CN-treated unstimulated and stimulated BV2 cells. Scale bar: 20 µm. LPS: 250 ng/ml for 24h. Concentrations refer to the amount of VP contained in each formulation (VP-CNC 1:10). *p<0.05, ***p<0.010, ****p<0.0001.

2.3.3. Improvement of Microglia Cell Viability by VP Nanoformulations

VP-CNC(-) and VP-CNC(+) dose-dependently increased cell viability under resting conditions, with a peak effect observed at 10 µg/mL, corresponding to VP 1 µg/mL (Figure 8A). Both treatments did not affect cell number under basal conditions (Figure 8B).

The nanocellulose formulations were also effective under proinflammatory conditions. Specifically, VP-CNC(-) and VP-CNC(+) restored cell viability reduced by LPS exposure (Figure 8C) and increased cell number to levels comparable to the control group (Figure 8D).

 doi:10.20944/preprints202512.0209.v1

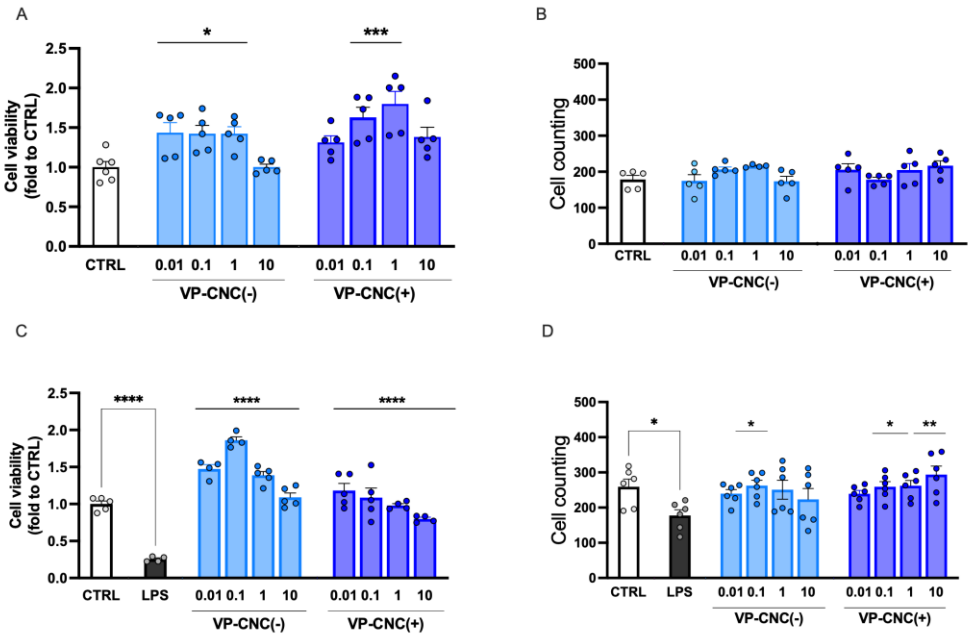

Figure 8. Effect of VP-CNC on cell viability. (A) VP-CNC(-) (0.01-1) and VP-CNC(+) (0.1-1) increase of cell viability at resting conditions. (B) Lack of effect on cell number by VP-CNC(-) and VP-CNC(+) (0.01-10) at steady state. LPS-stimulated cells showed a reduced cell viability (C) and number (D). Dose-dependently reversal of LPS-induced effect by VP-CNC(-) and VP-CNC(+) 0.01-10. LPS: 250 ng/ml for 24h. Concentrations refer to the amount of VP contained in each formulation (VP-CNC 1:10). *p<0.05, **p<0.01, ***p<0.001, ****p<0.0001.

2.3.4. VP-CNC Nanoformulation Effect on pERK1/2 and SIRT1 Levels

To evaluate the efficacy of the nanocellulose formulations on neuroinflammation markers, we assessed their effects on the expression of p-ERK1/2 (Figure 9A) and SIRT1 (Figure 9B). Treatment of LPS-stimulated cells with the highest effective doses of the formulations reduced p-ERK1/2 over-phosphorylation and increased SIRT1 levels. These results demonstrated that the VP-CNC formulations were comparably effective to unformulated VP. Importantly, these findings indicate the absence of confounding effects from the vehicle at the low VP doses and confirm CNC as a suitable drug-delivery system for plant cell culture–derived phytocomplexes.

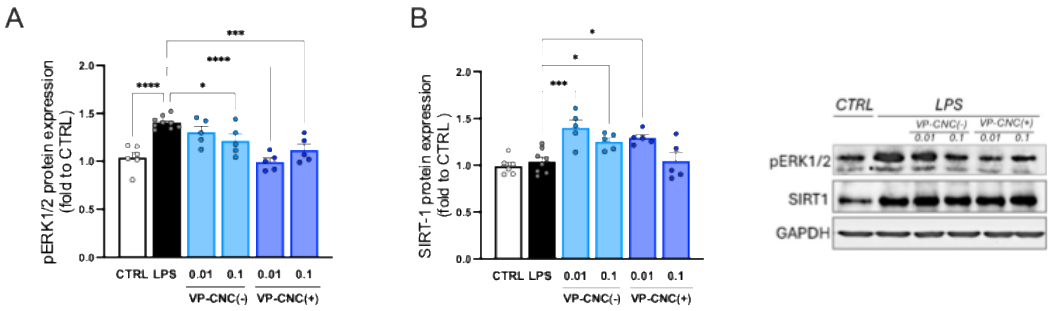

Figure 9. Effect of VP-CNC on neuroinflammation biomarkers. (A) Dose-dependent reduction of LPS-induced ERK1/2 over-phosphorylation. (B) VP-CNC increase of SIRT1 protein levels. Concentrations refer to the amount of VP contained in each formulation (VP-CNC 1:10). *p<0.05, ***p<0.001, ****p<0.0001.

3. Discussion

The levels of bioactive molecules in *V. vinifera* extracts vary widely due to numerous difficult-to-control factors, including seasonality, genetic differences among grape varieties, plant age, cultivation area, and the specific tissues used to produce the extracts [7,8]. This variability makes it

 doi:10.20944/preprints202512.0209.v1

challenging to obtain standardized *V. vinifera* derivatives with reproducible metabolite profiles. The considerable phytochemical variability of plant-derived extracts can also reduce their effectiveness. To overcome these limitations and ensure reproducibility and efficacy of biological activities, the present study utilized in vitro plant cell culture biotechnology. We investigated the pharmacological profile of a plant cell-derived *V. vinifera* L. phytocomplex in a model of microglia-mediated neuroinflammation.

Microglia support brain homeostasis during steady-state conditions [26]. Therefore, we first investigated the effects of VP on resting microglial cells. Treatment, while not altering the resting microglial phenotype, increased cell viability, suggesting a potential CNS-protective effect. In addition to their homeostatic role, microglia play a key role during injury or inflammatory insults, where their activation is intended to protect the CNS by promoting the release of inflammatory mediators and activating tissue repair mechanisms. However, prolonged and uncontrolled microglial activation can sustain neuroinflammation, exacerbating neuronal damage [27]. Accordingly, we tested the efficacy of VP in an in vitro model of neuroinflammation based on LPS stimulation of BV2 microglial cells [28]. Microglia are dynamic cells that, under inflammatory conditions, change their morphology from a resting to a proinflammatory phenotype. Morphological analysis showed that VP reversed the LPS-induced shift of BV2 cells from a short, round morphology to an elongated, large-sized phenotype. VP also restored the reduced cell viability and cell number under LPS stimulation, providing an initial indication of its anti-neuroinflammatory effect. These results are consistent with previous studies demonstrating anti-inflammatory effects of *Vitis vinifera* L. leaf extract in human keratinocytes [29] and murine macrophages [30] exposed to proinflammatory stimuli (i.e. tumor necrosis factor-α, LPS).

Activated microglia development and maintenance depend on constant engagement of the colony-stimulating factor 1 receptor (CSF1R), a receptor tyrosine kinase that transmits intracellular signals, such as activation of protein kinase B (AKT) and extracellular signal-regulated kinases (ERK), which promote microglial proliferation and survival [31]. In our model, neuroinflammation was induced in BV2 microglial cells by LPS exposure. LPS, by stimulating toll-like receptor 4 (TLR4), activates downstream MAPK signaling, which promotes the synthesis of proinflammatory mediators [32]. MAPKs are also involved in NF-κB activation, a transcription factor that drives microglial activation. Previous studies have reported that NF-κB is activated by MAPK ERK1/2 through mechanisms such as phosphorylation of NF-κB inhibitory factor IκBα and nuclear translocation of p65, contributing to a proinflammatory response [33,34]. VP reduced NF-κB activation and ERK1/2 hyperphosphorylation, further supporting its anti-neuroinflammatory mechanism.

Silent information regulator sirtuin 1 (SIRT1), a deacetylase member of the sirtuin family, regulates various biological functions and plays a key role in modulating inflammation [35]. Studies suggest that SIRT1 has strong anti-inflammatory effects by inhibiting the expression of factors involved in inflammatory pathways [35], including the NF-κB p65 subunit, thus inhibiting NF-κB activity [36]. SIRT1 may also limit NF-κB nuclear translocation and its DNA-binding ability [37]. Numerous anti-inflammatory drugs act by upregulating SIRT1 expression [38,39]. VP markedly increased microglial SIRT1 levels, consistently with an anti-neuroinflammatory activity. No significant variation in SIRT1 expression was observed following LPS exposure. This seemingly contradictory result may reflect the variability and context-dependent regulation of SIRT1 levels during inflammatory conditions [40].

The therapeutic effects of *V. vinifera* are attributed to its active constituents, primarily polyphenolic compounds. In particular, resveratrol, a stilbenoid, and viniferin, one of its derivatives, have been extensively studied for their antioxidant and anti-inflammatory properties. Their anti-inflammatory mechanisms are mainly associated with inhibition of both NF-κB activation and MAPK hyperphosphorylation [41]. Furthermore, resveratrol is a well-known SIRT1 activator [42,43]. Evidence also suggests that viniferins increase SIRT1 expression in vascular endothelial cells [44], while in adipocytes, ε-viniferin raises SIRT1 expression more effectively than resveratrol [45]. Thus,

 doi:10.20944/preprints202512.0209.v1

the pharmacological activity of VP appears to be related to its stilbenoid content, likely driven predominantly by viniferin.

The poor water solubility of VP may limit its potential clinical application due to the need for lipophilic solvents, which can induce cellular toxicity. To address this limitation, an innovative nano-formulation was employed.

Drug delivery systems have received considerable attention over the past decade because they offer several potential advantages, including reduced side effects, improved therapeutic efficacy, and lower effective doses [46]. Cellulose, a major natural plant component, possesses excellent renewability and biodegradability, making it a suitable, natural, non-toxic, and inexpensive material while maintaining good biological activity with minimal side effects. Technological advances have generated significant interest in nanocellulose [47] which has emerged as a promising "green" material for drug delivery applications [48].

We developed and investigated a water-disperdible, nanocellulose-based formulation containing VP that displayed biological activity comparable to unformulated VP, without inducing cellular toxicity. Moreover, the improved solubility enabled pharmacological effects at doses ten times lower than those required for the unformulated phytocomplex, indicating that this delivery system enhances the solubility and efficacy of natural compounds.

In conclusion, *V. vinifera* phytocomplex obtained from cell-culture suspensions represents an innovative and standardized ingredient with a strong safety profile, supported by a sustainable and clean production process. Plant cell-culture technology ensures controlled growth conditions for the selected and stable *V. vinifera* cell line, guaranteeing a high degree of standardization in the phytocomplex composition. This consistency in bioactive molecule content translates into reproducible biological efficacy.

Future studies will further explore the pharmacological activity of VP in models of neuroinflammation-mediated pathological conditions to assess its potential for clinical translation. Additionally, it will be important to dissect the contribution of individual constituents to identify the main active component(s) and determine whether synergistic interactions among VP stilbenoids enhance its overall biological effect.

4. Materials and Methods

4.1. Vitis vinifera L. Phytocomplex (VP) from Cell Culture Suspensions

A standardized and sustainable phytocomplex of *Vitis vinifera* L. (VP) was developed using plant cell culture technology. *V. vinifera* young plant was bought and certified from the nursery plant "Vivai Busatta", Camisano Vicentino, Vicenza, Italy. A stabilized and selected cell line specified on the biosynthesis of stilbenoids was obtained by dissected V. vinifera fruits (black grapes) using the following treatments in sequence: with 70% (v/v) ethanol (Honeywell, Wunstorfer Straβe 40, D-30926, Seelze, Germany) in water for about 1 min, followed by washing with sterile distilled water for 3 minutes. They were then washed in 2% (v/v) sodium hypochlorite solution (6–14% active chlorine, Merck KGaA, Darmstadt, Germany) and 0.1% (v/v) Tween 20 (Duchefa, Haarlem, The Netherlands) for 3 min and, finally, they were given at least 3 washes with sterile distilled water for 5 minutes each. After sanitization, the black grapes were cut into small pieces (explants) of sub-centimetric dimensions. The sanitized fragments of black grapes were deposited in several Petri dishes contained Gamborg B5 medium [49] supplemented with 20 g/L sucrose (Sudzucker AG, Manheim, Germany), 1 mg/L of naphthalenacetic acid (NAA) (Duchefa), 1 mg/L of indolacetic acid (IAA) (Duchefa), 1 mg/L of Kinetin (K) (Duchefa), 0.8% w/v of plant agar (Duchefa) and pH adjusted to 6.5 (G0 solid medium).

Petri dishes containing explants were incubated at 25±1°C in the dark. Calli were grown after 20 days of incubation and were subjected to subculture for 6 months (3 weeks of each subculture) until they became friable and homogeneous, with a constant growth rate (selected and stable *V. vinifera* cell line). The suspension cultures were obtained by transferring a part of selected calli (10% w/v) into 100 mL Erlenmeyer flasks containing 20 mL of G0 liquid culture medium (G0 without plant agar).

 doi:10.20944/preprints202512.0209.v1

The suspension cultures were incubated in a climatic growth room, in dark conditions, at 25±2°C on a rotary shaker in constant agitation at 120 rpm and were subcultivated in larger volume (from 0,1 L flasks to 3L flasks) every 7 days of fermentation. To produce large quantities of biomass, the suspension cultured was transferred and adapted to growth in a bioreactor of progressively increasing size (5L and 13L volume) with an amount of cell suspension inoculated into the liquid medium equal to 7% v/v.

To increase the total stilbenoid content, expressed as viniferin equivalent, after 7 days of fermentation in G0 liquid medium, 7% (v/v) of *V. vinifera* cell suspension was transferred to a final liquid medium (G0 containing 40g/L of sucrose). After 3 days of fermentation, 7.5 mg/L methyl jasmonate (Merck K GoA Darmstadt, Germany) and 25 mM β-cyclodextrin (Merck K GoA Darmstadt, Germany) were added to the suspension cell cultures.

After 14 days of growth in G0 final liquid medium at 25±2°C in a climatic growth room, in dark and on a rotary shaker in constant agitation at 120 rpm, the *V. vinifera* suspension cell cultures were filtered by a 50µm mesh filter to remove liquid culture medium. The collected cells were washed with twice volume of saline solution (0,9% w/w NaCl in sterile water) and added with citric acid 1% (w/w) and then homogenized with Ultra Turrax homogenizer at 15,000 rpm for 20 minutes. The biomass of homogenized cells was dried using a Mini Spray Dryer (BUCHI-B290) to obtain a powder of *V. vinifera* standardized phytocomplex (VP) with high content of total stilbenoids expressed as viniferin equivalent.

4.2. UPLC-DAD Analysis of Vitis vinifera L. Standardized Phytocomplex (VP)

UPLC-DAD was used to quantify the total stilbenoids present in VP. To prepare the sample, 25 mg of VP were dissolved in a 50:50 (v/v) methanol–water mixture. The suspension was vortexed for 30 seconds and then sonicated for 15 minutes in an ice bath to ensure thorough extraction. After sonication, the mixture was centrifuged at 13,000 rpm for 10 minutes at 6 °C. The resulting supernatant was collected, diluted 1:10 with the same methanol–water mixture, and passed through a 0.22 µm membrane filter before UPLC-DAD analysis. Four separate extractions and analyses were performed to confirm reproducibility.

Chromatographic separation was carried out on a UPLC system equipped with an Acquity UPLC BEH C18 column (1.7 µm, 2.1 × 100 mm) and a VanGuard BEH C18 pre-column (1.7 µm, 2.1 × 5 mm), both from Waters. The UPLC-DAD platform (Ultra Performance Liquid Chromatography with Diode Array Detection) included a Binary Solvent Manager I-Class module and a Sample Manager-FTN I-Class autosampler, connected to a PDA eλ detector. Data were acquired and processed using Empower 3 software (Waters, Feature Release 4).

The mobile phase consisted of solvent A (water with 0.1% formic acid) and solvent B (acetonitrile with 0.1% formic acid). The run started with 90% solvent A at a constant flow rate of 0.2 mL/min, while the column temperature was maintained at 30 °C.

Quantification of total stilbenoids was performed by monitoring the chromatograms at 330 nm, using a calibration curve prepared with a commercial (+)-epsilon-viniferin standard (purity ≥ 97.2%, Extrasynthase, France). Data acquisition and processing were carried out using Empower 3 software.

4.3. Synthesis CNC (+)

Procedure, with minor changes, from Liu, Y. et al. [50].

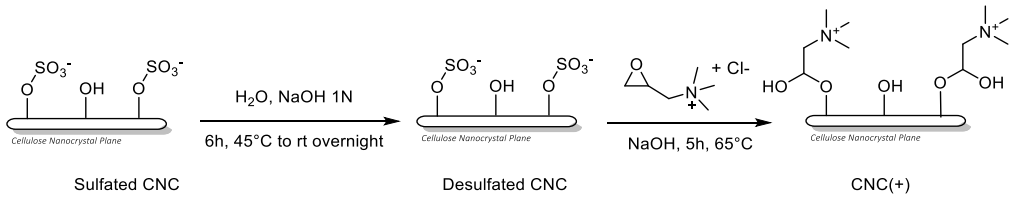

 doi:10.20944/preprints202512.0209.v1

Sodium hydroxide powder (400 mg) was added to a suspension of sulfated cellulose nanocrystals (Sulfated CNC, commercially available CelluForce NCC® NCV100-NASD90; 500 mg, 5 wt%) in water (10 mL) to obtain a 1 N NaOH solution. The reaction mixture was stirred at 65°C for 6h and subsequently at room temperature overnight. After dialysis against Milli-Q water until neutral pH, the dispersion was concentrated to obtain a suspension of desulfated CNC (424 mg, 8.2 wt%) in water. Next, NaOH (21 mg, 5% by weight of CNC) was added and the reaction mixture was stirred for 30 minutes at room temperature. Glycidyltrimethylammonium chloride (894 mg, 5.9 mmol) was then added in a molar ratio 2.5:1 respect to desulfated CNC. The reaction mixture was stirred at 65°C for 5h. Finally, the mixture was dialyzed against MilliQ water for 7 days and lyophilized to afford CNC (+) (400 mg) as a fluffy white solid.

Elemental Analysis: *C 40.15%, H 5.91%, N 0.53%, S 0.00%.* ***ζ-potential:*** *(48.91 ± 3.81) mV.*

4.4. Preparation of VP-CNC Nanoformulations

VP-CNC(-) and VP-CNC(+) 10:1 (100 mg : 10 mg) were used. In a 5 mL stainless-steel jar were added Sulfated CNC (100 mg) or CNC (+) (100 mg) and VP (10 mg). The powders were grinded at 10 Hz for 15 minutes using three stainless steel balls (⌀= 0.5 cm).

VP-CNC(+) ***ζ-potential:*** (+36.03 ± 2.91) mV; VP-CNC(-) ***ζ-potential:*** (-34.69 ± 3.13) mV.

4.5. BV2 Cell Culture

BV2 murine immortalized microglial cells (mouse, C57BL/6, brain, microglial cells, Tema Ricerca, Genova, Italy; 16–20 passages) were thawed and kept in culture in a 75 cm^2 flask in a medium containing RPMI with the addition of 10% of heat-inactivated (56°C, 30 min) fetal bovine serum (FBS, Gibco, Milan, Italy) 1% glutamine, and a 1% penicillin–streptomycin solution (Merck, Darmstadt, Germany). Cells were cultured at 37°C and 5% CO_2 with daily medium change until confluence (70–80%). Trypan blue staining was used for cell counting.

4.6. Treatments

VP was dissolved in a vehicle composed of bidistilled water and DMSO (1:1) to obtain a homogeneous 1 mg/mL dispersion. The dispersion was then diluted with RPMI to obtain final concentrations of 0.1, 1, 10, and 100 mg/mL. VP-CNC(–) and VP-CNC(+) were dissolved in bidistilled water to obtain a 1 mg/mL solution, corresponding to 100 μg/mL of VP. The VP-CNC solutions were then diluted with RPMI to obtain concentrations of 0.1, 1, 10, and 100 μg/mL, corresponding to 0.01, 0.1, 1, and 10 μg/mL VP, respectively. Cells were treated with vehicle or VP, VP-CNC(–), and VP-CNC(+) for 4 hours and then, to induce neuroinflammation, BV2 cells were stimulated for 24 h with a bacterial lipopolysaccharide from Gram- (LPS, 250 ng/mL Merck, Darmstadt, Germany).

4.7. Sulforhodamine B (SRB) Assay

Cell viability was assessed by the sulforhodamine B (SRB) assay [51]. Cells (2 x 10^4 cells in 200 mL) were seeded in 96-well plates incubated with vehicle, VP, VP-CNC(-) and VP-CNC(+) (0.1 - 1 - 10 -100 μg/ml) in the presence or absence of LPS stimulation. Cells were fixed in 50% trichloroacetic acid at 4°C for 1 h, treated with a solution of SRB 4 mg/mL in 1% acetic acid and incubated for 30 min at room temperature. Wells were washed four times with 1% acetic acid, added with 200 mL of TRIS HCl solution (pH 10) and incubated for 5 min with shaking. Absorbance was determined using a microplate reader at 570 nm. All treatments were carried out in six technical replicates across three independent experiments, and cell viability was expressed relative to the mean value of the control group.

4.8. Cell Counting and Morphology

Cell counting and measurement of the cell diameter and soma surface area were performed by experimenter's blind to the cell culture conditions on images taken by Leica DM IL LED FLUO optical

 doi:10.20944/preprints202512.0209.v1

microscope and analyzed through the ImageJ program, used for the quantification of total cell number, soma diameter and area. The cells were counted per mm^2 microscopic area in at least ten randomly selected fields. For each treatment group three independent experiments were performed [52].

4.9. Western Blot Analysis

BV2 cells were lysed using a lysis buffer. The insoluble pellet was separated by centrifugation (12,000 × g for 30 min, 4 °C), and the total protein concentration in the supernatant was measured using the Bradford colorimetric method (Merck, Milan, Italy) [51]. Protein samples (20 μg) were separated on 10% SDS-PAGE and then blotted onto Midi Nitrocellulose membranes using a Trans-Blot Turbo Transfer Starter System (Bio-Rad Laboratories, Milan, Italy). Blots were incubated overnight at 4 °C with primary antibodies against pERK1/2 (1:1000, Cell Signaling Technology, Danvers, MA, USA), SIRT1 (1:1000, Santa Cruz Biotechnology, Dallas, TX, USA), NFκB p65 (1:1000, Santa Cruz Biotechnology), and p-NFκB p65 (1:500, Santa Cruz Biotechnology). After being washed with PBS containing 0.1% Tween, the nitrocellulose membranes were incubated with goat anti-rabbit or anti-mouse horseradish peroxidase–conjugated secondary antibodies (1:3000, Jackson ImmunoResearch Labs, West Grove, PA, USA) for 2 h at room temperature (RT; 20–22 °C). After washing, blots were developed using an enhanced chemiluminescence detection system (ChemiDoc Imaging Systems, Bio-Rad, Milan, Italy), and signal intensity (pixels/mm^2) was quantified using ImageJ 2.14 (NIH, Bethesda, MD, USA). Exposure and development times were standardized for all blots. For each sample, signal intensity was normalized to GAPDH (1:1000, Santa Cruz Biotechnology), and the acquired images were quantified using ImageJ 2.14 software.

4.10. Statistical Analysis

The results are expressed as mean ± SEM. A one-way analysis of variance (ANOVA) followed by the Tukey post hoc test was used for statistical analysis. Student's t test was used when necessary. Values of $p < 0.05$ were considered significant. Outliers were identified and excluded from each experimental set using the ROUT method [53]. The software GraphPad Prism version 10.6.0 (GraphPad Software, San Diego, CA, USA) was used in all statistical analyses.

5. Conclusions

This study aimed to investigate the anti-neuroinflammatory properties of Vitis vinifera L., the common grapevine, a valuable source of antioxidant bioactive molecules such as stilbenes (e.g., resveratrol, viniferin) and flavonoids. However, the substantial variability of conventional V. vinifera extracts limits the production of standardized derivatives with consistent metabolite profiles. To obtain standardized products, technologies capable of ensuring reproducible metabolite production, eliminating seasonal and geographical variability, and improving environmental sustainability while reducing contamination risks are required. For this purpose, we employed in vitro plant cell culture technology to generate uniform, contaminant-free plant material. Additionally, to address the common issue of poor bioavailability of natural products, we developed a water-soluble nanocellulose-based formulation of the phytocomplex.

We found that both the characterized plant cell culture–derived V. vinifera phytocomplex and its nanocellulose formulation attenuated microglia-mediated neuroinflammation by reducing the proinflammatory phenotype, preserving cell viability, suppressing NF-κB activation and ERK1/2 phosphorylation, and enhancing SIRT1 expression.

These findings confirm the therapeutic potential of V. vinifera L. as an anti-neuroinflammatory intervention, underscore the value of plant cell culture technology for producing standardized and reproducible phytocomplexes, and highlight nanocellulose as a safe and innovative delivery system. Overall, our results support biotechnology-driven strategies to improve the consistency and efficacy

 doi:10.20944/preprints202512.0209.v1

of natural products for potential clinical applications in neuroinflammatory and neurodegenerative conditions.

Author Contributions: Conceptualization, N.G., GP, O.B., S.C., B.R. and C.G.; formal analysis, G.V, C.S., O.B. and C.G.; investigation, G.V, C.S., S.Q., O.B., S.C., B.R., G.B., E.B. and C.G.; writing—original draft preparation, N.G. and G.P..; writing—review and editing, N.G.., S.C. and B.R.; visualization, C.S., O.B. and C.G.; supervision, N.G and G.P.; project administration, N.G..; funding acquisition, N.G and G.P. All authors have read and agreed to the published version of the manuscript.

Funding: This research was funded by: #NEXTGENERATIONEU (NGEU) and funded by the Ministry of University and Research (MUR), National Recovery and Resilience Plan (NRRP), project MNESYS (PE0000006)—A Multiscale integrated approach to the study of the nervous system in health and disease (DN. 1553 11.10.2022); Ministry of Enterprise and Made in Italy, Innovation Agreement 18/10/2023, the PLANTFORM project, grant number F/310143/01-03/X56.

Institutional Review Board Statement: Not applicable.

Informed Consent Statement: Not applicable.

Data Availability Statement: The data presented in this study are available on request from the corresponding author.

Acknowledgments: B.R., G.B., S.C., E.B thank the "Progetto Dipartimenti di Eccellenza 2023–2027", allocated to the Department of Chemistry "Ugo Schiff").

Conflicts of Interest: The authors declare no conflicts of interest.

Abbreviations

The following abbreviations are used in this manuscript:

AKT	activation of protein kinase B
CNC	cellulose nanocrystal
CNS	central nervous system
CSF1R	colony-stimulating factor 1 receptor
ERK	extracellular signal-regulated kinases
LPS	bacterial lipopolysaccharide from Gram-
MAPK	mitogen activated protein kinase
NF-κB	nuclear factor κB
RNS	reactive nitrogen species
ROS	reactive oxygen species
SIRT1	Silent information regulator sirtuin 1
TLR4	toll-like receptor 4
VP	*Vitis vinifera* L. phytocomplex

References

1. Waisman, A.; Liblau, R.S.; Becher, B. Innate and Adaptive Immune Responses in the CNS. *Lancet Neurol* **2015**, *14*, 945–955, doi:10.1016/S1474-4422(15)00141-6.
2. Adamu, A.; Li, S.; Gao, F.; Xue, G. The Role of Neuroinflammation in Neurodegenerative Diseases: Current Understanding and Future Therapeutic Targets. *Front Aging Neurosci* **2024**, *16*, doi:10.3389/FNAGI.2024.1347987.
3. DiSabato, D.J.; Quan, N.; Godbout, J.P. Neuroinflammation: The Devil Is in the Details. *J Neurochem* **2016**, *139 Suppl 2*, 136–153, doi:10.1111/JNC.13607.
4. Kölliker-Frers, R.; Udovin, L.; Otero-Losada, M.; Kobiec, T.; Herrera, M.I.; Palacios, J.; Razzitte, G.; Capani, F. Neuroinflammation: An Integrating Overview of Reactive-Neuroimmune Cell Interactions in Health and Disease. *Mediators Inflamm* **2021**, *2021*, doi:10.1155/2021/9999146.

5. Ajoolabady, A.; Kim, B.; Abdulkhaliq, A.A.; Ren, J.; Bahijri, S.; Tuomilehto, J.; Borai, A.; Khan, J.; Pratico, D. Dual Role of Microglia in Neuroinflammation and Neurodegenerative Diseases. *Neurobiol Dis* **2025**, *216*, 107133, doi:10.1016/j.nbd.2025.107133.
6. Li, Q.; Barres, B.A. Microglia and Macrophages in Brain Homeostasis and Disease. *Nat Rev Immunol* **2018**, *18*, 225–242, doi:10.1038/NRI.2017.125.
7. Qin, J.; Ma, Z.; Chen, X.; Shu, S. Microglia Activation in Central Nervous System Disorders: A Review of Recent Mechanistic Investigations and Development Efforts. *Front Neurol* **2023**, *14*, doi:10.3389/FNEUR.2023.1103416.
8. Kwon, H.S.; Koh, S.H. Neuroinflammation in Neurodegenerative Disorders: The Roles of Microglia and Astrocytes. *Transl Neurodegener* **2020**, *9*, doi:10.1186/S40035-020-00221-2.
9. Gao, C.; Jiang, J.; Tan, Y.; Chen, S. Microglia in Neurodegenerative Diseases: Mechanism and Potential Therapeutic Targets. *Signal Transduct Target Ther* **2023**, *8*, doi:10.1038/S41392-023-01588-0.
10. Shi, F.D.; Yong, V.W. Neuroinflammation across Neurological Diseases. *Science* **2025**, *388*, doi:10.1126/SCIENCE.ADX0043.
11. Goufo, P.; Singh, R.K.; Cortez, I. A Reference List of Phenolic Compounds (Including Stilbenes) in Grapevine (Vitis Vinifera L.) Roots, Woods, Canes, Stems, and Leaves. *Antioxidants (Basel)* **2020**, *9*, doi:10.3390/ANTIOX9050398.
12. Zhou, D.D.; Li, J.; Xiong, R.G.; Saimaiti, A.; Huang, S.Y.; Wu, S.X.; Yang, Z.J.; Shang, A.; Zhao, C.N.; Gan, R.Y.; et al. Bioactive Compounds, Health Benefits and Food Applications of Grape. *Foods* **2022**, *11*, doi:10.3390/FOODS11182755.
13. Chen, H.; Yang, J.; Deng, X.; Lei, Y.; Xie, S.; Guo, S.; Ren, R.; Li, J.; Zhang, Z.; Xu, T. Foliar-Sprayed Manganese Sulfate Improves Flavonoid Content in Grape Berry Skin of Cabernet Sauvignon (Vitis Vinifera L.) Growing on Alkaline Soil and Wine Chromatic Characteristics. *Food Chem* **2020**, *314*, doi:10.1016/j.foodchem.2020.126182.
14. Tetik, F.; Civelek, S.; Cakilcioglu, U. Traditional Uses of Some Medicinal Plants in Malatya (Turkey). *J Ethnopharmacol* **2013**, *146*, 331–346, doi:10.1016/j.jep.2012.12.054.
15. Ishtiaq, M.; Mahmood, A.; Maqbool, M. Indigenous Knowledge of Medicinal Plants from Sudhanoti District (AJK), Pakistan. *J Ethnopharmacol* **2015**, *168*, 201–207, doi:10.1016/j.jep.2015.01.054.
16. Nassiri-Asl, M.; Hosseinzadeh, H. Review of the Pharmacological Effects of Vitis Vinifera (Grape) and Its Bioactive Constituents: An Update. *Phytother Res* **2016**, *30*, 1392–1403, doi:10.1002/PTR.5644.
17. Lakshmi, B.V.S.; Sudhakar, M.; Anisha, M. Neuroprotective Role of Hydroalcoholic Extract of Vitis Vinifera against Aluminium-Induced Oxidative Stress in Rat Brain. *Neurotoxicology* **2014**, *41*, 73–79, doi:10.1016/j.neuro.2014.01.003.
18. Pazos-Tomas, C.C.; Cruz-Venegas, A.; Pérez-Santiago, A.D.; Sánchez-Medina, M.A.; Matías-Pérez, D.; García-Montalvo, I.A. Vitis Vinifera: An Alternative for the Prevention of Neurodegenerative Diseases. *J Oleo Sci* **2020**, *69*, 1147–1161, doi:10.5650/JOS.ESS20109.
19. Krasteva, G.; Georgiev, V.; Pavlov, A. Recent Applications of Plant Cell Culture Technology in Cosmetics and Foods. *Eng Life Sci* **2020**, *21*, 68–76, doi:10.1002/ELSC.202000078.
20. Georgiev, V.; Slavov, A.; Vasileva, I.; Pavlov, A. Plant Cell Culture as Emerging Technology for Production of Active Cosmetic Ingredients. *Eng Life Sci* **2018**, *18*, 779–798, doi:10.1002/ELSC.201800066.
21. Biermann, O.; Hädicke, E.; Koltzenburg, S.; Müller-Plathe, F.; Müller-Plathe, F.; Biermann, Dipl.-C.O.; Hädicke, E.; Koltzenburg, S. Hydrophilicity and Lipophilicity of Cellulose Crystal Surfaces. *Angew. Chem. Int. Ed* **2001**, *40*, doi:10.1002/1521-3773(20011015)40:20.
22. Lindman, B.; Medronho, B.; Alves, L.; Norgren, M.; Nordenskiöld, L. Hydrophobic Interactions Control the Self-Assembly of DNA and Cellulose. *Q Rev Biophys* **2021**, *54*, doi:10.1017/S0033583521000019.
23. Kumar, R.; Chauhan, S. Cellulose Nanocrystals Based Delivery Vehicles for Anticancer Agent Curcumin. *Int J Biol Macromol* **2022**, *221*, 842–864, doi:10.1016/J.IJBIOMAC.2022.09.077.
24. Mazeau, K.; Wyszomirski, M. Modelling of Congo Red Adsorption on the Hydrophobic Surface of Cellulose Using Molecular Dynamics. *Cellulose 2012 19:5* **2012**, *19*, 1495–1506, doi:10.1007/S10570-012-9757-6.

 doi:10.20944/preprints202512.0209.v1

25. Piras, C.C.; Fernández-Prieto, S.; De Borggraeve, W.M. Ball Milling: A Green Technology for the Preparation and Functionalisation of Nanocellulose Derivatives. *Nanoscale Adv* **2019**, *1*, 937–947, doi:10.1039/C8NA00238J.
26. Van Hove, H.; De Feo, D.; Greter, M.; Becher, B. Central Nervous System Macrophages in Health and Disease. *Annu Rev Immunol* **2025**, *43*, 589–613, doi:10.1146/ANNUREV-IMMUNOL-082423-041334.
27. Colonna, M.; Butovsky, O. Microglia Function in the Central Nervous System During Health and Neurodegeneration. *Annu Rev Immunol* **2017**, *35*, 441–468, doi:10.1146/ANNUREV-IMMUNOL-051116-052358.
28. Borgonetti, V.; Anceschi, L.; Brighenti, V.; Corsi, L.; Governa, P.; Manetti, F.; Pellati, F.; Galeotti, N. Cannabidiol-Rich Non-Psychotropic Cannabis Sativa L. Oils Attenuate Peripheral Neuropathy Symptoms by Regulation of CB2-Mediated Microglial Neuroinflammation. *Phytother Res* **2022**, doi:10.1002/PTR.7710.
29. Sangiovanni, E.; Di Lorenzo, C.; Piazza, S.; Manzoni, Y.; Brunelli, C.; Fumagalli, M.; Magnavacca, A.; Martinelli, G.; Colombo, F.; Casiraghi, A.; et al. Vitis Vinifera L. Leaf Extract Inhibits In Vitro Mediators of Inflammation and Oxidative Stress Involved in Inflammatory-Based Skin Diseases. *Antioxidants (Basel)* **2019**, *8*, doi:10.3390/ANTIOX8050134.
30. Acero, N.; Manrique, J.; Muñoz-Mingarro, D.; Martínez Solís, I.; Bosch, F. Vitis Vinifera L. Leaves as a Source of Phenolic Compounds with Anti-Inflammatory and Antioxidant Potential. *Antioxidants (Basel)* **2025**, *14*, doi:10.3390/ANTIOX14030279.
31. Dai, X.M.; Ryan, G.R.; Hapel, A.J.; Dominguez, M.G.; Russell, R.G.; Kapp, S.; Sylvestre, V.; Stanley, E.R. Targeted Disruption of the Mouse Colony-Stimulating Factor 1 Receptor Gene Results in Osteopetrosis, Mononuclear Phagocyte Deficiency, Increased Primitive Progenitor Cell Frequencies, and Reproductive Defects. *Blood* **2002**, *99*, 111–120, doi:10.1182/BLOOD.V99.1.111.
32. Arthur, J.S.C.; Ley, S.C. Mitogen-Activated Protein Kinases in Innate Immunity. *Nat Rev Immunol* **2013**, *13*, 679–692, doi:10.1038/NRI3495.
33. Liu, P.; Li, Y.; Wang, W.; Bai, Y.; Jia, H.; Yuan, Z.; Yang, Z. Role and Mechanisms of the NF-κB Signaling Pathway in Various Developmental Processes. *Biomedicine & Pharmacotherapy* **2022**, *153*, 113513, doi:10.1016/J.BIOPHA.2022.113513.
34. Gandhi, D.; Bhandari, S.; Maity, S.; Mahapatra, S.K.; Rajasekaran, S. Activation of ERK/NF-KB Pathways Contributes to the Inflammatory Response in Epithelial Cells and Macrophages Following Manganese Exposure. *Biol Trace Elem Res* **2025**, *203*, 127–138, doi:10.1007/S12011-024-04154-Z.
35. Yang, Y.; Liu, Y.; Wang, Y.; Chao, Y.; Zhang, J.; Jia, Y.; Tie, J.; Hu, D. Regulation of SIRT1 and Its Roles in Inflammation. *Front Immunol* **2022**, *13*, doi:10.3389/FIMMU.2022.831168.
36. Yeung, F.; Hoberg, J.E.; Ramsey, C.S.; Keller, M.D.; Jones, D.R.; Frye, R.A.; Mayo, M.W. Modulation of NF-KappaB-Dependent Transcription and Cell Survival by the SIRT1 Deacetylase. *EMBO J* **2004**, *23*, 2369–2380, doi:10.1038/SJ.EMBOJ.7600244.
37. Lei, M.; Wang, J.G.; Xiao, D.M.; Fan, M.; Wang, D.P.; Xiong, J.Y.; Chen, Y.; Ding, Y.; Liu, S.L. Resveratrol Inhibits Interleukin 1β-Mediated Inducible Nitric Oxide Synthase Expression in Articular Chondrocytes by Activating SIRT1 and Thereby Suppressing Nuclear Factor-KB Activity. *Eur J Pharmacol* **2012**, *674*, 73–79, doi:10.1016/j.ejphar.2011.10.015.
38. Hu, T.; Fan, X.; Ma, L.; Liu, J.; Chang, Y.; Yang, P.; Qiu, S.; Chen, T.; Yang, L.; Liu, Z. TIM4-TIM1 Interaction Modulates Th2 Pattern Inflammation through Enhancing SIRT1 Expression. *Int J Mol Med* **2017**, *40*, 1504–1510, doi:10.3892/IJMM.2017.3150.
39. Li, Y.; Liu, T.; Li, Y.; Han, D.; Hong, J.; Yang, N.; He, J.; Peng, R.; Mi, X.; Kuang, C.; et al. Baicalin Ameliorates Cognitive Impairment and Protects Microglia from LPS-Induced Neuroinflammation via the SIRT1/HMGB1 Pathway. *Oxid Med Cell Longev* **2020**, *2020*, doi:10.1155/2020/4751349.
40. Sun, H.; Li, D.; Wei, C.; Liu, L.; Xin, Z.; Gao, H.; Gao, R. The Relationship between SIRT1 and Inflammation: A Systematic Review and Meta-Analysis. *Front Immunol* **2024**, *15*, 1465849, doi:10.3389/FIMMU.2024.1465849/BIBTEX.
41. Al-Khayri, J.M.; Mascarenhas, R.; Harish, H.M.; Gowda, Y.; Lakshmaiah, V.V.; Nagella, P.; Al-Mssallem, M.Q.; Alessa, F.M.; Almaghasla, M.I.; Rezk, A.A.S. Stilbenes, a Versatile Class of Natural Metabolites for Inflammation-An Overview. *Molecules* **2023**, *28*, doi:10.3390/MOLECULES28093786.

 doi:10.20944/preprints202512.0209.v1

42. Howitz, K.T.; Bitterman, K.J.; Cohen, H.Y.; Lamming, D.W.; Lavu, S.; Wood, J.G.; Zipkin, R.E.; Chung, P.; Kisielewski, A.; Zhang, L.L.; et al. Small Molecule Activators of Sirtuins Extend Saccharomyces Cerevisiae Lifespan. *Nature* **2003**, *425*, 191–196, doi:10.1038/nature01960.
43. Rogina, B.; Tissenbaum, H.A. SIRT1, Resveratrol and Aging. *Front Genet* **2024**, *15*, 1393181, doi:10.3389/FGENE.2024.1393181/BIBTEX.
44. Wu, C.W.; Nakamoto, Y.; Hisatome, T.; Yoshida, S.; Miyazaki, H. Resveratrol and Its Dimers ε-Viniferin and δ-Viniferin in Red Wine Protect Vascular Endothelial Cells by a Similar Mechanism with Different Potency and Efficacy. *Kaohsiung J Med Sci* **2020**, *36*, 535–542, doi:10.1002/KJM2.12199.
45. Hung, M.W.; Wu, C.W.; Kokubu, D.; Yoshida, S.; Miyazaki, H. ε-Viniferin Is More Effective than Resveratrol in Promoting Favorable Adipocyte Differentiation with Enhanced Adiponectin Expression and Decreased Lipid Accumulation. *Food Sci Technol Res* **2019**, *25*, 817–826, doi:10.3136/FSTR.25.817.
46. Hasan, N.; Rahman, L.; Kim, S.H.; Cao, J.; Arjuna, A.; Lallo, S.; Jhun, B.H.; Yoo, J.W. Recent Advances of Nanocellulose in Drug Delivery Systems. *Journal of Pharmaceutical Investigation 2020 50:6* **2020**, *50*, 553–572, doi:10.1007/S40005-020-00499-4.
47. Karimian, A.; Parsian, H.; Majidinia, M.; Rahimi, M.; Mir, S.M.; Samadi Kafil, H.; Shafiei-Irannejad, V.; Kheyrollah, M.; Ostadi, H.; Yousefi, B. Nanocrystalline Cellulose: Preparation, Physicochemical Properties, and Applications in Drug Delivery Systems. *Int J Biol Macromol* **2019**, *133*, 850–859, doi:10.1016/j.ijbiomac.2019.04.117.
48. Huo, Y.; Liu, Y.; Xia, M.; Du, H.; Lin, Z.; Li, B.; Liu, H. Nanocellulose-Based Composite Materials Used in Drug Delivery Systems. *Polymers 2022, Vol. 14, Page 2648* **2022**, *14*, 2648, doi:10.3390/POLYM14132648.
49. Gamborg, O.L.; Miller, R.A.; Ojima, K. Nutrient Requirements of Suspension Cultures of Soybean Root Cells. *Exp Cell Res* **1968**, *50*, 151–158, doi:10.1016/0014-4827(68)90403-5.
50. Liu, Y.; Li, M.; Qiao, M.; Ren, X.; Huang, T.S.; Buschle-Diller, G. Antibacterial Membranes Based on Chitosan and Quaternary Ammonium Salts Modified Nanocrystalline Cellulose. *Polym Adv Technol* **2017**, *28*, 1629–1635, doi:10.1002/PAT.4032;PAGE:STRING:ARTICLE/CHAPTER.
51. Borgonetti, V.; Pressi, G.; Bertaiola, O.; Guarnerio, C.; Mandrone, M.; Chiocchio, I.; Galeotti, N. Attenuation of Neuroinflammation in Microglia Cells by Extracts with High Content of Rosmarinic Acid from in Vitro Cultured Melissa Officinalis L. Cells. *J Pharm Biomed Anal* **2022**, *220*, doi:10.1016/J.JPBA.2022.114969.
52. Videtta, G.; Sasia, C.; Galeotti, N. High Rosmarinic Acid Content Melissa Officinalis L. Phytocomplex Modulates Microglia Neuroinflammation Induced by High Glucose. *Antioxidants (Basel)* **2025**, *14*, doi:10.3390/ANTIOX14020161.
53. Motulsky, H.J.; Brown, R.E. Detecting Outliers When Fitting Data with Nonlinear Regression - a New Method Based on Robust Nonlinear Regression and the False Discovery Rate. *BMC Bioinformatics* **2006**, *7*, doi:10.1186/1471-2105-7-123.